

A LOW POWER 46 ns 2⁵⁶ kbit CMOS STATIC
RAM WITH DYNAMIC DOUBLE WORD LINE

TAKAYASU SAKURAI, JUNICHI MATSUNAGA, MITSUO ISOBE,
TAKAYUKI OHTANI, KAZUHIRO SAWADA, AKIRA AONO, HIROSHI NOZAWA,
TETSUYA IIZUKA and SUSUMU KOHYAMA

Reprinted from IEEE Journal of Solid-State Circuits, Vol. SC-19, No. 5, October 1984

A Low Power 46 ns 256 kbit CMOS Static RAM with Dynamic Double Word Line

TAKAYASU SAKURAI, MEMBER, IEEE, JUNICHI MATSUNAGA, MITSUO ISOBE, TAKAYUKI OHTANI, KAZUHIRO SAWADA, AKIRA AONO, HIROSHI NOZAWA, TETSUYA IIZUKA, MEMBER, IEEE, AND SUSUMU KOHYAMA, MEMBER, IEEE

Abstract—A fast and low power 32K×8 bit CMOS static RAM with high-resistive polyload 4-transistor cell is developed utilizing a dynamic double word line (DDWL) scheme, a combination of automatic power down (APD) circuitry, and double word line (DWL) structure. The DDWL, together with bit line and sense line equilibration reduces the core area delay time and operating power to about 1/2 and 1/15 that of a conventional device, respectively. A newly developed fault-tolerant circuitry improves fabrication yield without degrading the access time. As for a fabrication process, an advanced 1.2 μm p-well CMOS technology is developed to realize the ULSI RAM, integrating 1.6 million elements on a $6.68 \times 8.86 \text{ mm}^2$ chip. The RAM offers, typically, 46 ns access time, 10 mW operating, and 30 μW standby power.

I. INTRODUCTION

THE memory capacity of CMOS static RAM's has been quadrupled every two years during the last four generations. This rate of increase is faster than dynamic RAM's. In 1982 64 kbit CMOS static RAM's (C/SRAM's) were announced [1]–[3], and in this paper a 256 kbit CMOS static RAM with high-resistive polyload 4-transistor cells is reported, a herald of a ULSI's (ultra large scale integrations), including 1.6 million elements on a chip.

The advantages of a CMOS static RAM over a dynamic RAM lie in its high speed, low power, and highly reliable operation, without any complex refresh controls. These salient features of CMOS static RAM's are positively pursued in this 256 kbit C/SRAM, resulting in 46 ns access time and 10 mW power dissipation at 1 MHz.

Key technologies for realizing the high performance C/SRAM are summarized in Table I, from the standpoint of both circuitry and processing. In the table, the purpose and effects are made clear.

The fast and low power operation is achieved by using a unique word line scheme, called dynamic double word line (DDWL). The DDWL is a combination of a double word line (DWL) structure [4]–[6] and an automatic power down

TABLE I
KEY TECHNOLOGIES FOR HIGH SPEED AND LOW POWER 1.6 MILLION ELEMENT ULSI RAM

TECHNOLOGY	PURPOSE	
	HIGH SPEED	LOW POWER
1. Double Word Line Structure: Double Metal 16 Sections	Y	Y
2. Automatic Power Down Function ATD Circuitry Word Line Pulse Wider than Access Time		Y
3. BL and SL Equilibration: ATD Circuitry	Y	
4. Reliable 5V 1.2 μm Device Process: C-SEPOX Isolation SEPOS LDD	Y	

(APD) scheme. In order to implement the APD function, a word line is activated dynamically by a pulse wider than the access time. The DDWL cuts down the operating power at 1 MHz to about 1/15 that of a conventional device. Address transition detectors (ATD's) [1] are incorporated in the RAM to generate the activation pulse for the APD function. This ATD also provides a means for equilibration of bit lines (BL's) and sense lines (SL's), which turn out to be very effective in realizing a fast access time. The equilibration circuitry, together with the DDWL scheme, reduces the access time to about one-half, compared with a conventional RAM. As for yield optimization, a new redundancy circuitry has been proposed which does not sacrifice the fast access time.

An advanced 1.2 μm p-well CMOS process with double polysilicon and double aluminum was developed to integrate 1.6 million elements on a chip of reasonable size, with a cell size of $11 \times 13.5 \mu\text{m}^2$. The high packing density of this level is achieved with the help of bird's beak free C-SEPOX (CMOS selective polysilicon oxidation) isolation technology [7]. Since peripheral circuitry speeds up as the supply voltage increases, 5 V operation is preferred over lower voltages for high speed operation. Reliable 5 V operation of submicron channel length MOSFET's was demonstrated by using an LDD (lightly doped drain)

Manuscript received March 1, 1984; revised May 16, 1984.

T. Sakurai, J. Matsunaga, M. Isobe, T. Ohtani, K. Sawada, H. Nozawa, T. Iizuka, and S. Kohyama are with Semiconductor Device Engineering Laboratory, Toshiba Corporation, Kawasaki, 210 Japan.

A. Aono is with Toshiba Microcomputer Engineering Corporation, Kawasaki, 210 Japan.

structure fabricated by SEPOS (self-defined polysilicon sidewall structure) process [8].

In Sections II and III, the process and circuit technologies are described in detail. Resulted performances and other features of the 256 kbit C/SRAM are treated in Section IV. Section V concludes the paper.

II. 1.2 μm CMOS PROCESS TECHNOLOGY

An advanced 1.2 μm p-well CMOS process is developed to fabricate the RAM. A p-well process, where all memory cells are embedded in the well, is chosen to mitigate soft errors. The potential barrier of the p-well reflects the long-term drift component of alpha-particle induced current. For a short-term drift component, so-called funneling, an RC time-constant isolation technique can be effective [9]. The cell layout technique also reduces the soft error rate associated with the drift component [10].

Design rules of the 256 kbit C/SRAM are listed in Table II, where comparison with the previous generation 64 kbit C/SRAM [1] are made. 1.5 μm n^+-n^+ spacing is achieved by using bird's beak free C-SEPOX isolation technology, the details of which are reported in [7]. As seen from the table, the effective channel length of an n-channel MOSFET is 0.8 μm . A conventional n-channel MOSFET of this submicron channel region suffers from the notorious hot carrier problem. A newly developed SEPOS LDD process [8] has been successfully applied to make reliable submicron MOSFET's for 5 V operation. The SEPOS process offers better controllability and wider margins and results in very small degradation of drain conductivity with respect to conventional transistors. The reliable 5 V operation of submicron MOSFET's, together with double-metal interconnects, which decrease RC delay of word lines and jumper lines, are indispensable for a fast circuit operation.

The double-level polysilicon process has a small chip size, which contributes not only to higher gross productivity but also to reduction of parasitic capacitance. The first level poly layer is used for the gates of MOSFET's, while the second layer, whose sheet resistivity is over 100 $\text{G}\Omega/\square$, serves as the high-resistive polyloads for the memory cells, realizing a low standby power of 30 μW and enabling battery backup of stored data. The second layer is also used for V_{dd} supply lines for memory cells, where the sheet resistivity is lowered to less than 50 Ω/\square through a selective doping.

III. CIRCUIT DESIGN

Fig. 1 shows the trend of delay components in scaled-down C/SRAM's. As seen from the figure, the core area delay time, namely WL, BL, and SL delay, dominates the access time. This is basically because the peripheral circuitry speeds up by the scaling, but the capacitance of bus lines cannot be scaled since the number of memory cells for one bus line is doubled. Some remedies should be used to achieve high speed operation of scaled C/SRAM's. Our

TABLE II
DESIGN RULES OF 64 AND 256 kbit CMOS STATIC RAM

PARAMETERS	64K-CMOS RAM	256K-CMOS RAM
PROCESS	DOUBLE-LEVEL POLY-Si SINGLE-LEVEL Al	DOUBLE-LEVEL POLY-Si DOUBLE-LEVEL Al
GATE LENGTH (NMOS)	2.0 μm	1.2 μm
GATE LENGTH (PMOS)	2.2 μm	1.5 μm
GATE OXIDE THICKNESS	450 \AA	250 \AA
JUNCTION DEPTH (N ⁺)	0.25 μm	0.20 μm
JUNCTION DEPTH (P ⁺)	0.50 μm	0.35 μm
DIFFUSION (WIDTH/SPACING)	1.6 $\mu\text{m}/2.6 \mu\text{m}$	1.2 $\mu\text{m}/1.5 \mu\text{m}$
POLY-Si (WIDTH/SPACING)	2 $\mu\text{m}/2 \mu\text{m}$	1.2 $\mu\text{m}/1.2 \mu\text{m}$
1st Al (WIDTH/SPACING)	2 $\mu\text{m}/2 \mu\text{m}$	1.2 $\mu\text{m}/1.6 \mu\text{m}$
1st CONTACT HOLE	2 $\mu\text{m}/2 \mu\text{m}$	1.2 $\mu\text{m}/1.2 \mu\text{m}$
2nd Al (WIDTH/SPACING)	—	2.0 $\mu\text{m}/2.0 \mu\text{m}$
2nd CONTACT HOLE	—	2.0 $\mu\text{m}/2.0 \mu\text{m}$

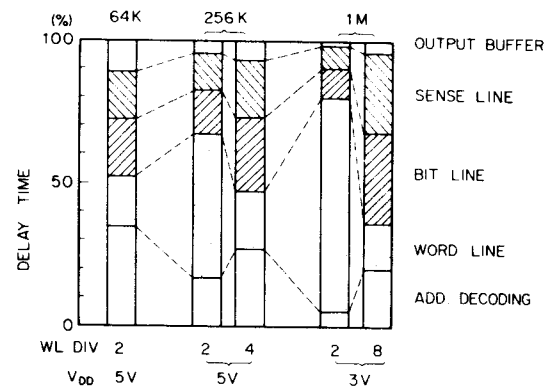


Fig. 1. Trends of delay component in scaled-down C/SRAM's. The trends are calculated by assuming a simple scaling law with a fit at 64 kbit C/SRAM. Mobility degradation due to the scaling is obtained from measured data of up to 0.8 μm MOSFET's. Two-dimensional effects are taken into account in estimating capacitances [11]. Output capacitance is set to zero because it depends on the external circumstances.

solutions are DWL structure for WL delay, and equilibration for BL and SL delay, which will be discussed in Sections III-A and III-D.

The scaled RAM also suffers from large power dissipation because the number of the activated cells have been doubled, if simple shrinkage is adopted. The DDWL is one of the solutions for this problem. As for a yield problem, a new redundancy circuitry is devised, which is treated in Section III-E.

A. Double Word Line Structure

The basic configuration of DDWL is shown in Fig. 2. Word lines are doubly placed, namely main word lines (MWL's) and section word lines (SWL's) [4]–[6]. Since an MWL is not directly connected to memory cells, capacitance of the MWL is relatively small, reducing the WL delay. The MWL is made by the second aluminum layer, which also reduces the delay. Low power dissipation is expected because only one SWL is selected at a time, and consequently only a small number of memory cells are activated. From a viewpoint of delay time and power dissipation, the greater the number of sections, the better the performance is. However, the chip area of the SWL

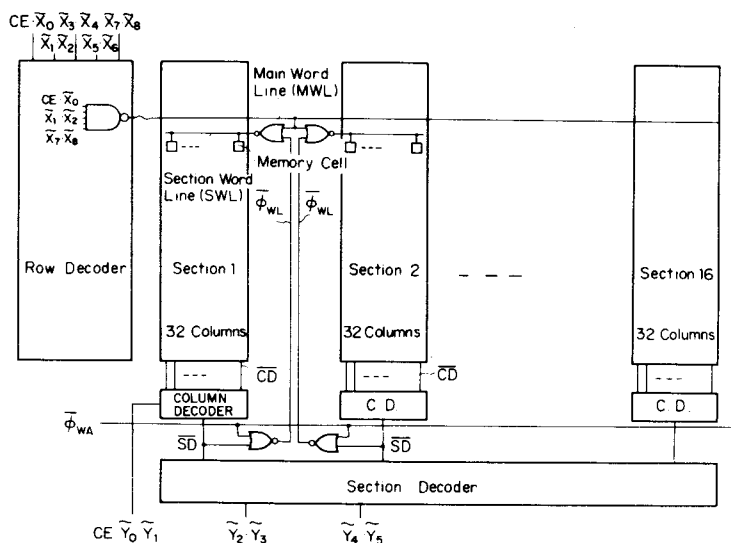


Fig. 2. Basic configuration of the dynamic double word line (DDWL) scheme.

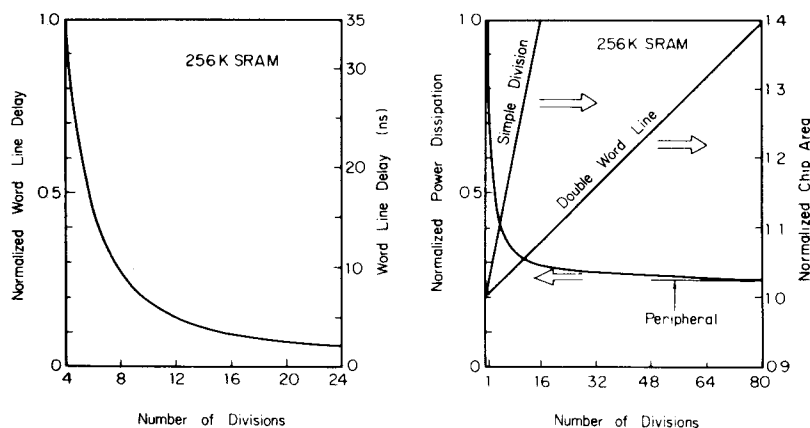


Fig. 3. Tradeoff among delay, power, and area for double word line structure. Step voltage is incident at a word line drive point. Section word line delay is estimated by using 3-step pi ladder circuit, which turned out to be the best circuit to simulate RC lines [14].

select NOR circuits, taking 2.5 cell areas each, increases linearly as the number of sections increases. Therefore, the number of sections cannot be set too large, although the area overhead is much smaller than a simple division of WL's, where many row decoders are required. This tradeoff is illustrated in Fig. 3. In the present device, the number of sections chosen is 16, where the delay and power improvement are saturated. At this point, the delay and power reduction are about 30 ns and 30 percent, respectively, with the chip area being the same, compared with the 4-divided conventional poly-WL structure.

Predecoding of address signals [12] is also effective in reducing the access time.

B. Automatic Power Down Function

A rough sketch of internal waveforms and a schematic diagram of a core part are shown in Fig. 4. When an address changes, address transition detectors (ATD's) create two classes of clocks, namely equilibration clocks and

activation clocks. The equilibration clocks (ϕ_{BE} and ϕ_{ME}) are explained in Section III-D. The activation clocks consist of sense amplifier activation clocks (ϕ_{SA} and ϕ_{MA}) and a word line activation clock (ϕ_{WA}). The clock-controlled word lines are one of the main features of the DDWL scheme. These activation clocks have a pulse width wider than an access time, and control sense amplifiers and SWL's so as to cut all the dc path in the RAM after a read operation is over. Consequently, no dc power is consumed. This is the principle of the automatic power down (APD) function. Since the activation pulse width is set at about 100 ns, the supply current depends linearly on the operation frequency below 10 MHz, as shown in Fig. 5. The activation pulse should have a width of 1.5–2.0 times the access time in order to salvage the slowest bits and to improve yield. A typical operation frequency for low power portable systems, where battery operation is a must, is around 1 MHz. The operation power at 1 MHz is reduced to about 1/10 that of a conventional RAM through the action of the APD function only.

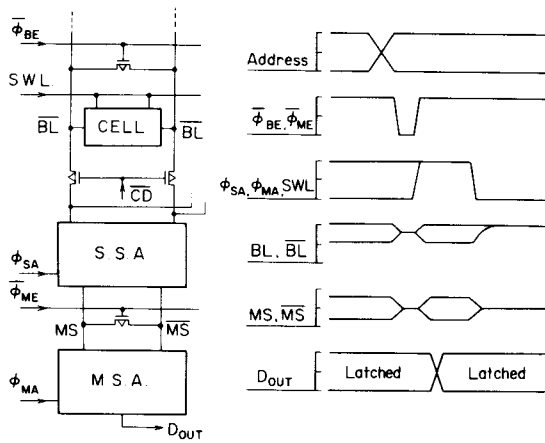


Fig. 4. A rough sketch of internal waveforms and a schematic diagram of a core part.

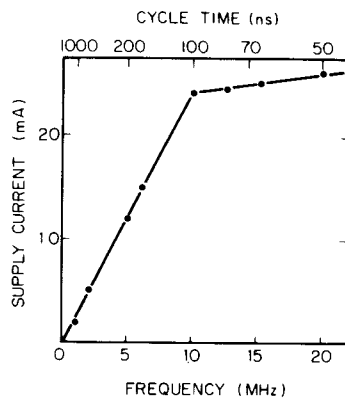


Fig. 5. Measured supply current versus operation frequency. Since the activation pulse width is set to about 100 ns, the supply current depends linearly on the operation frequency below 10 MHz. The measurement is carried out with no load and a supplied voltage of 5 V. The read cycle is repeated with output "1" and "0" alternated every cycle time.

C. Sense Amplifiers and Double Sense Line Structure

The two-stage current-mirror sense amplifiers shown in Fig. 6 are used to realize fast sensing. In the case of a latch-type amplifier commonly used in dynamic RAM's, the timing of the latch clock is very critical. The latch timing should come after the slowest memory cell pushes out the stored information to bit lines, unless a malfunction should occur. However, if the latch timing is very late, it degrades the access time. In the current-mirror amplifier, which is essentially static, there is no tradeoff between clock timing and access time. That is, yield and access time are always optimized. Moreover, the relatively small voltage swing of the bit lines is indispensable for fast equilibration. It should be noted that, although the RAM is internally controlled by clocks, the timing variation of these clocks does not give rise to malfunctions of the device.

Corresponding to the DWL, hierarchical structure is also adopted for sense lines, namely section sense lines (SS's) and main sense lines (MS's). This double sense line structure reduces the capacitance of MS lines and as a result the sensing delay.

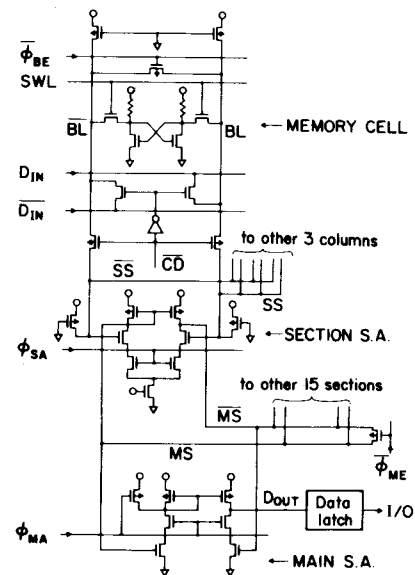


Fig. 6. Two-stage current-mirror sense amplifiers and double sense line structure.

D. Equilibration Scheme

Before stored information is read out from memory cells, bit lines and sense lines are equilibrated by using the equilibration clocks ϕ_{BE} and ϕ_{ME} (see Figs. 4 and 6). The equilibration is done in parallel with address decoding, exerting no delay in the sensing operation [13]. Instead, 20 ns access time reduction by the equilibration is observed by a computer simulation. This is because considerable time is required to cancel the effect of previous data if there is no equilibration.

E. Redundancy

Spare cells are widely included in VLSI RAM's [1]–[3] to improve fabrication yield. In 8 bit I/O RAM's, the spare row approach has more freedom in cell replacement and/or less overhead for redundancy circuitry than the spare column approach. Therefore the spare row approach is used in this RAM.

Simple calculation is carried out to determine the number of spare rows that optimizes the gross-yield product. Let Y_0 be the normalized initial yield. Y_0 is unity when all rows are safe. Then the probability that one row is safe (P_1) is $Y_0^{(1/N)}$, where N is the total number of normal rows ($N = 512$ for a 256 kbit C/SRAM). The normalized yield (Y) by using S spare rows is the probability that at least N rows are good in $(N + S)$ rows. Y should be multiplied by a factor if column fault mode and peripheral fault mode are considered, but for spare row number optimization this factor can be omitted.

$$Y = \sum_{j=0}^S \binom{N+S}{j} P_1^j (1-P_1)^{N+S-j} \cdot (1-P_1)^j$$

However, gross productivity decreases as S increases due to overhead area consumed by redundancy circuits. To take this effect into account, Y is multiplied by $1/(1 + v_1)$.

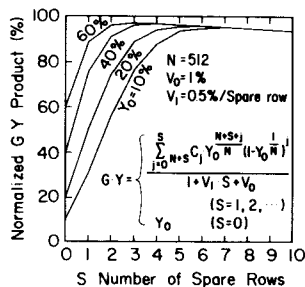


Fig. 7. Normalized gross-yield product versus number of spare rows. Four spare rows are adopted as optimum.

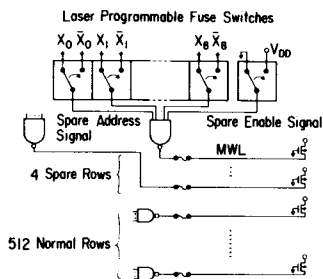


Fig. 8. Redundancy circuitry. The switches in the figure are constructed by using similar techniques as those in [1]. Disabling of a normal row is done not by an electrical signal but by blowing a fuse, which is good for the fast access time.

$S + v_0$), where v_1 stands for the overhead area factor to include one spare row and accompanying redundancy circuits, and v_0 for the overhead area factor to incorporate the redundancy scheme itself. The resulted expression for gross-yield product ($G \cdot Y$) is shown in Fig. 7, together with $G \cdot Y$ curves for this device. Consequently, four spare rows are chosen.

The new redundancy circuitry is shown in Fig. 8. When a spare row is selected, the corresponding normal row should be disabled. Conventionally, this disabling process is executed by an electrical signal. The signal is generated after deciding if an input address is one of the repaired addresses. This process is rather slow. Since the row selection should be done after the deselection, unless row multi-select should happen, a conventional redundancy scheme would degrade the access time. In the new circuit, the disabling is done by blowing off the poly fuse and no sacrifice of access time occurs. Moreover, if a replaced spare row malfunctions, then the spare row can be replaced again by another spare row.

IV. PERFORMANCE AND OTHER FEATURES

The internal waveforms of the RAM in read operation are shown in Fig. 9. The measured data are obtained by a strobo SEM tester. Voltage swings of BL and MS are fitted to computer-simulated values because the strobo SEM tester does not provide an absolute value of a node voltage but only a relative value. In the measurement, I/O pins are not loaded with an external capacitance and the suspected I/O voltage response for 100 pF output capacitance is indicated by a broken line. The waveforms of the clocks

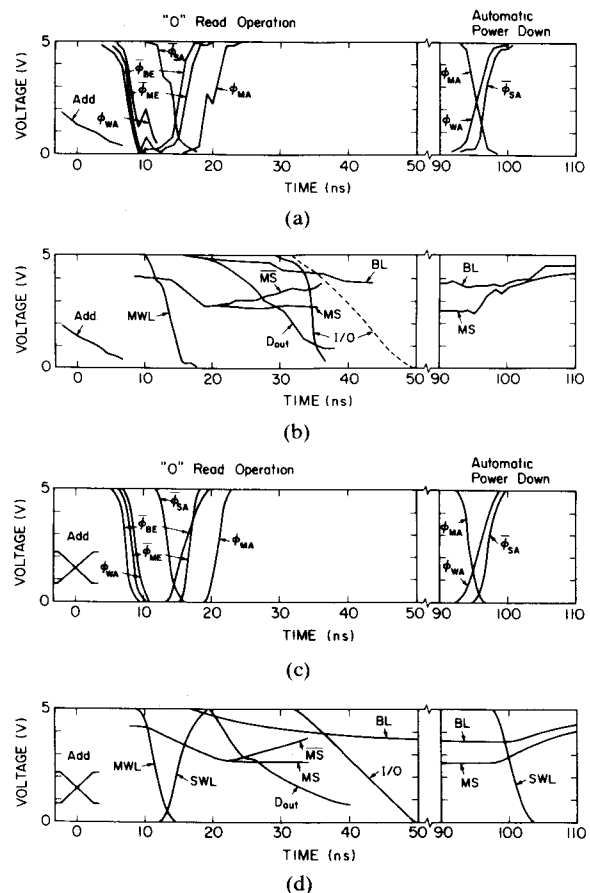


Fig. 9. Internal waveforms of the RAM. (a) Measured clocks. (b) Measured bus line signals. (c) Simulated clocks. (d) Simulated bus line signals. The measurement is carried out by a strobo SEM tester, which is a very useful tool for examining the debugging ULSI C/SRAM's. The simulation is done by SPICE2.

and bus lines are plotted in separate figures for easier reading. As seen from the figures, the power down function is initiated at about 95 ns after an address changes. As a whole, the measured waveforms are in good agreement with the simulation and the successful realization of the above-mentioned design concepts has been assured. This agreement also suggests the effectiveness of the SPICE2 circuit simulation program in ULSI CMOS RAM design. Fig. 10 is a Schmo plot of the present device, showing 46 ns access time at 5 V.

Fig. 11 is a chip microphotograph. As seen from the photograph, the cell area occupies about 70 percent of the total chip. This high value of occupation is attributed to the 1.2 μm process, the DWL structure, and the laser blown fuse redundancy circuits. The white vertical lines in the cell area are the place where ϕ_{WL} lines are located.

The typical RAM characteristics are tabulated in Table III. The 256 kbit C/SRAM is internally clocked by the ATD, but fully asynchronous externally. So that no severe control of address skews is required, in contrast with dynamic RAM's where careful on-board design should be done for RAS and CAS timing.

I/O buffers are TTL compatible with three-state output. The package is a standard 600 mil 28 pin DIP and the pin

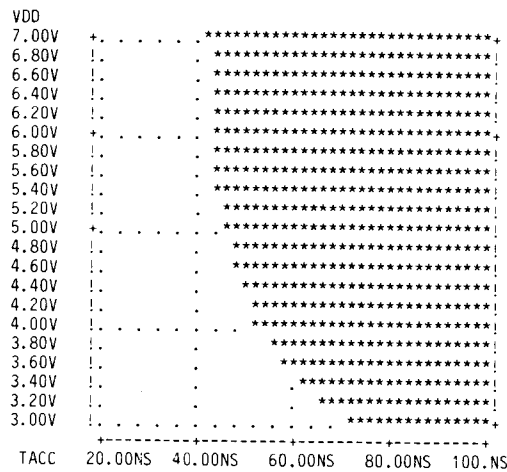


Fig. 10. Schmoo plot of the present device, showing 46 ns access time at 5 V.

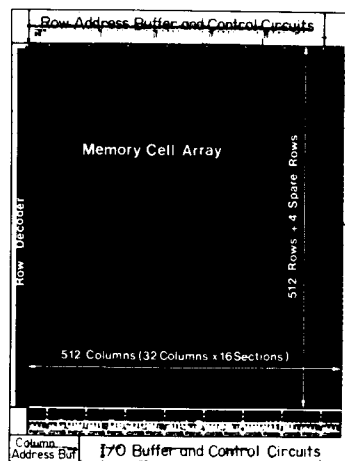


Fig. 11. Microphotograph of 256 kbit CMOS static RAM. The chip size is $6.68 \times 8.86 \text{ mm}^2$.

configuration is shown in Fig. 12. This pin configuration is compatible to 64 kbit CMOS static RAM's.

V. CONCLUSION

A fast and low power $32\text{K} \times 8$ bit CMOS static RAM with high-resistive polyload memory cell has been developed. An advanced $1.2 \mu\text{m}$ p-well CMOS process with bird's beak free C-SEPOX isolation technology was applied for integrating 1.6 million elements on a $6.68 \times 8.86 \text{ mm}^2$ chip. Double poly and double aluminum process contributes to the high packing density and fast circuit operation. The fast circuit operation is also supported by submicron channel length MOSFET's fabricated by SEPOS LDD process, which enables reliable 5 V operation.

As for the circuit design, the double word line (DWL) structure together with bit line and sense line equilibration, reduced the core area delay time drastically and a typical access time of 46 ns was achieved.

The dynamic double word line (DDWL) scheme, a combination of automatic power down (APD) circuitry and DWL structure was successfully applied to realize 10 mW

TABLE III
TYPICAL RAM CHARACTERISTICS

OPERATION	FULLY ASYNCHRONOUS (ADDRESS ACTIVATED CLOCKED OPERATION) AUTO POWER DOWN FUNCTION
ORGANIZATION	32K WORDS \times 8 BIT
REDUNDANCY	4 SPARE ROWS
CHIP SIZE	$6.68 \times 8.86 \text{ mm}^2$
CELL SIZE	$11 \times 13.5 \mu\text{m}^2$
I/O INTERFACE	TTL COMPATIBLE
ADDRESS ACCESS TIME	46 ns
ACTIVE POWER	10 mW (1 MHz)
STANDBY POWER	30 μW
PACKAGE	STANDARD 28PIN DIP

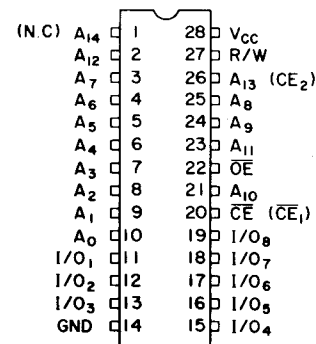


Fig. 12. Pin configuration of 256 kbit CMOS static RAM. The pin configuration is compatible with 64 kbit CMOS static RAM, whose pin configuration is shown in parentheses.

at 1 MHz and 120 mW at 10 MHz operation. Considering the resulting high speed and low power operation of the 256 kbit C/SRAM, the DDWL scheme seems to be very promising for future ULSI memories, not only for static RAM's but also for ROM's, EPROM's, and EEPROM's.

Address transition detectors (ATD's) are incorporated in the RAM to generate equilibration and activation control clocks. The use of ATD's can be a mainstream technique of ULSI static RAM's to achieve internally clocked but externally fully asynchronous operation, that is, to build a high performance and easy-to-use RAM.

For cost minimization, newly developed redundancy circuits with 4 spare rows are used, which optimize yield without degrading the fast access time.

ACKNOWLEDGMENT

The authors would like to express their thanks to K. Shimizu, Y. Nishi, and Y. Uchida for encouragement throughout the work, and N. Matsukawa, H. Kaneko, H. Momose, M. Saito, H. Shibata, and T. Maeda for their every endeavor in processing, and M. Ishikawa, K. Sato, and K. Tamaru for their support in the phase of evaluation and simulation.

REFERENCES

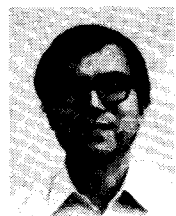
- [1] S. Kojishi, J. Matsunaga, T. Ohtani, M. Sekine, M. Isobe, T. Iizuka, Y. Uchida, and S. Kohyama, "A 64 kbit CMOS RAM," in *ISSCC Dig. Tech. Papers*, Feb. 1982, pp. 258-259.
- [2] K. Ochiai, K. Hashimoto, H. Yasuda, M. Masuda, H. Nozawa, and S. Kohyama, "A 15 nW standby power 64 kbit CMOS RAM," in *ISSCC Dig. Tech. Papers*, Feb. 1982, pp. 260-261.
- [3] O. Minato, T. Masuhara, T. Sasaki, and T. Hayashida, "A hi-CMOS II 8K \times 8-bit static RAM," in *ISSCC Dig. Tech. Papers*, Feb. 1982, pp. 256-257.
- [4] T. Sakurai, T. Furuyama, and T. Iizuka, "Methods for analyzing a word line delay and their applications," *Community Solid-State Device IECE Jap.*, vol. SSD82, p. 15, Oct. 1982.
- [5] M. Yoshimoto, K. Anami, H. Shinohara, T. Yoshihara, H. Takagi, S. Nagano, S. Kayano, and T. Nakano, "A 64K full CMOS RAM with divided word line structure," in *ISSCC Dig. Tech. Papers*, Feb. 1983, pp. 58-59.
- [6] T. Sakurai and T. Iizuka, "Double word line and bit line structure for VLSI RAM's," in *Proc. 15th Conf. Solid-State Devices and Materials*, 1983, pp. 269-272.
- [7] N. Matsukawa, H. Nozawa, J. Matsunaga, and S. Kohyama, "Selective polysilicon oxidation technology for VLSI isolation," *IEEE Trans. Electron Devices*, vol. ED-29, pp. 561-567, Apr. 1982.
- [8] J. Miyamoto, S. Saitoh, H. Momose, H. Shibata, K. Kanzaki, and S. Kohyama, "A 1.0 μ m n-well CMOS/bipolar technology for VLSI circuits," in *Tech. Dig. IEDM*, 1983, pp. 63-66.
- [9] T. Iizuka and T. Sakurai, "CR isolated cell for soft error prevention," in *Dig. Tech. Papers, 1983 Symp. VLSI Technol.*, pp. 70-71.
- [10] K. Anami, M. Yoshimoto, H. Shinohara, Y. Harata, and T. Nakano, "A 35 ns 16K NMOS static RAM," in *ISSCC Dig. Tech. Papers*, Feb. 1982, pp. 250-251.
- [11] T. Sakurai and K. Tamaru, "Simple formulas for two- and three-dimensional capacitances," *IEEE Trans. Electron Devices*, vol. ED-30, Feb. 1983, pp. 183-185.
- [12] T. Iizuka, K. Ochiai, T. Ohtani, T. Kondo, and S. Kohyama, "A fully static 16K bulk CMOS RAM," in *ISSCC Dig. Tech. Papers*, Feb. 1980, pp. 226-227.
- [13] K. Hardee and R. Sud, "A fault-tolerant 30 ns/375 mW 16K \times 1 NMOS static RAM," *IEEE J. Solid-State Circuits*, vol. SC-16, pp. 435-443, Oct. 1981.
- [14] T. Sakurai, "Approximation of wiring delay in MOSFET LSI," *IEEE J. Solid-State Circuits*, vol. SC-18, pp. 418-426, Aug. 1983.



Takayasu Sakurai (S'77-M'78) was born in Tokyo, Japan, on January 10, 1954. He received the B.S., M.S., and Ph.D. degrees in electronic engineering from the University of Tokyo, Tokyo, Japan, in 1976, 1978, and 1981, respectively. His Ph.D. work is on the electronic structure of Si-SiO₂ interface.

In 1981 he joined the Toshiba Semiconductor Device Engineering Laboratory, Toshiba Corporation, Kawasaki, Japan, where he was engaged in the research and development of CMOS dynamic and 64K and 256K static memories. During development, he also worked on modeling of wiring capacitance and delay, new soft-error free memory cell, and new memory architectures.

Dr. Sakurai is a member of the Institute of Electronics and Communication Engineers of Japan and Japan Society of Applied Physics.



Junichi Matsunaga was born in Oita, Japan, on May 11, 1948. He received the B.S. degree in physics from Kyoto University, Kyoto, Japan, in 1972, and the M.S. degree from the University of Tokyo, Tokyo, Japan, in 1974.

In 1974 he joined the Toshiba Research and Development Center, Toshiba Corporation, Kawasaki, Japan. He has been engaged in the development of dynamic RAM's and microprocessors, particularly in the electrical characterization of process technologies. He is currently

working with the Semiconductor Device Engineering Laboratory, Toshiba Corporation, and is working on process technology and device physics for higher packing density static MOS RAM's, especially CMOS RAM's.

Mr. Matsunaga is a member of the Japan Society of Applied Physics.



Mitsuo Isobe was born in Niigata Prefecture, Japan, on January 3, 1948. He received the B.S. and M.S. degrees in electrical engineering from Waseda University, Tokyo, Japan, in 1971 and 1973, respectively.

He joined the Toshiba Research and Development Center, Toshiba Corporation, Kawasaki, Japan, in 1973, where he has worked on the research and development of NMOS/SOS LSI. From 1979 to 1981, he was engaged in the research and development of CMOS/SOS memory LSI, and is currently working on CMOS/bulk memory VLSI at the Semiconductor Device Engineering Laboratory, Toshiba Corporation, Kawasaki, Japan.



Takayuki Ohtani was born in Tokyo, Japan, on June 13, 1952. He received the B.S. and M.S. degrees in electronic engineering from Waseda University, Tokyo, Japan, in 1975 and 1977, respectively.

In 1977 he joined the Toshiba Research and Development Center. In 1979 he joined the Semiconductor Device Engineering Laboratory, Toshiba Corporation, Kawasaki, Japan. He has been engaged in the research and development of CMOS memories. He developed 16K, 64K, and

256K CMOS static RAM's.

Mr. Ohtani is a member of the Institute of Electronics and Communication Engineers of Japan.



Kazuhiro Sawada was born in Hyogo, Japan, on March 25, 1957. He received the B.S. and M.S. degrees in electronic engineering from Keio University, Tokyo, Japan, in 1980 and 1982, respectively.

In 1982 he joined the Toshiba Semiconductor Device Engineering Laboratory, Toshiba Corporation, Kawasaki, Japan, where he was engaged in the research and development of CMOS static memories.

Mr. Sawada is a member of the Institute of Electronics and Communication Engineers of Japan.



Akira Aono was born in Tokyo, Japan, on November 8, 1958. He received the B.S. degree in electronic engineering from Musashi Institute of Technology, Tokyo, Japan, in 1982.

In 1982 he joined the Toshiba Microcomputer Engineering Corporation, Kawasaki, Japan. He is engaged in the research and development of CMOS static memories.



Hiroshi Nozawa was born in Kanagawa Prefecture, Japan, on December 10, 1947. He received the B.S. and M.S. degrees in metal science and technology from Kyoto University, Kyoto, Japan, in 1970 and 1972, respectively.

In 1972 he joined the Toshiba Research and Development Center, Toshiba Corporation, Kawasaki, Japan, where he was engaged in the development of EPROM processes. Since 1979 he has been engaged in the development of high-density CMOS memory processes and isolation technology. He is currently the Manager of the Advanced CMOS Technology Group in the Semiconductor Device Engineering Laboratory at Toshiba.

Mr. Nozawa is a member of the Japan Society of Applied Physics and the Institute of Electronics and Communication Engineers of Japan.



Tetsuya Iizuka (M'77) was born in Ibaraki, Japan, on April 17, 1947. He received the B.S. degree in applied physics, the M.S. and Ph.D. degrees in electrical engineering from the University of Tokyo, Tokyo, Japan, in 1970, 1972, and 1975, respectively.

In 1975 he joined the Toshiba Research and Development Center, Toshiba Corporation, Kawasaki, Japan, where he was engaged in research on I^2L and CMOS/SOS devices and in the development of dynamic RAM testing

method. In 1979 he transferred to a newly organized laboratory, the Semiconductor Device Engineering Laboratory (SDEL), Toshiba Corporation, where he developed first generations of 16K, 64K, and 256K CMOS SRAM's. In 1981 he stayed for one year at the Integrated Circuit Laboratory, Hewlett-Packard, Palo Alto, CA, as a Visiting Engineer. He worked on CMOS latch-up modeling and bird's beak free isolated MOST analysis. He is currently Manager of the Advanced SRAM, EPROM, and EEROM Design Group of the SDEL, Toshiba Corporation, Kawasaki, Japan.

Dr. Iizuka is a member of the Institute of Electrical and Communication Engineers of Japan.



Susumu Kohyama was born in Japan on February 26, 1943. He received the B.S. and M.S. degrees, both in applied physics, from the University of Tokyo, Tokyo, Japan in 1966 and 1968, respectively.

In 1969 he joined the Toshiba Research and Development Center, Toshiba Corporation, Kawasaki, Japan. Since 1973 he has been engaged in the development of advanced MOS technologies, including CCD, NMOS, and CMOS, mainly for memory applications. Since

1979, he led series of CMOS memory development, as well as advanced CMOS technology research and development, as Manager at the Semiconductor Device Engineering Laboratory. He is currently the Senior Manager of the Logic Device Engineering Department, Integrated Circuits Division, and his current interests are in the area of CMOS technologies for logic VLSI applications, including custom and semicustom VLSI design.

Mr. Kohyama is a member of the Japan Society of Applied Physics and the Physical Society of Japan.